

Characterization of Sub-50 nm Line Array Structures with Angle Resolved Multiple Wavelength Scatterometry

Michael Kotelyanskii, Fei Shen, Gary Jiang RUDOLPH TECHNOLOGIES, NJ
Benjamin Bunday ISMI, TX

Presented at the SPIE 2008

ABSTRACT

In the sub-90 nm technology nodes, optical metrology techniques are essential for process control of gate formation steps, from lithography to etch layers such as gate, trench, and dielectric interconnect layers and to spacers and straining layer depositions. Conventionally^{5,6,7}, optical metrology is based on measurements of periodic line or hole arrays (i.e., gratings) using spectroscopic ellipsometers or polarized reflectometers, collecting data across wide wavelength spectra at a single angle of incidence. In this paper, we present results of measurements on periodic etched amorphous-Si gate line arrays using focused beam ellipsometry (FBE), illuminating at three discrete laser wavelengths while data is collected over angles of incidence ranging from 45° to 65°. Results on thoroughly characterized samples representative of 65 and 45 nm technology are presented. These samples include a variety of both line critical dimensions (CDs) (from 18–50 nm) and line pitches (from 200–700nm) for dense and isolated lines arrays. We discuss precision and accuracy in terms of total measurement uncertainty; spot size, navigation, and tool matching are also presented. FBE-based metrology will meet current process control requirements within a substantial margin.

INTRODUCTION

Optical scatterometry techniques find more and more applications in the semiconductor manufacturing process. Compared to direct characterization techniques such as scanning electron microscopy (SEM) or atomic force microscopy (AFM), they are faster and nondestructive, allowing users to incorporate them in real-time process

control. Optical scatterometry has been almost exclusively used with spectroscopic ellipsometry in planar diffraction geometry, i.e., with the grating ridges perpendicular to the incidence plane⁵. Here we discuss a scatterometry approach that uses simultaneous angle of incidence resolved measurements at a discrete set of wavelengths to characterize a-Si periodic line grating arrays. We analyze and compare performance in the traditional non-conical configuration (lines are perpendicular to the incidence plane of the ellipsometer) with a conical configuration when lines are parallel to the incidence plane. Even though the latter is a conical diffraction configuration, the Jones matrix of the periodic line grating sample is still diagonal, and sample properties can be represented in terms of the ratio ($r_{pp}/r_{ss} = \tan(\Psi) \exp(i\Delta)$) of the p- and s- polarization reflection coefficients². When lines are not parallel or orthogonal to the incidence plane, off-diagonal Jones matrix elements r_{ps} are in general non-zero and must be accounted for separately. two-parameter recipe to 1–2Mbytes for a typical three-parameter library, and up to 50Mbytes for five-parameter libraries.

ANGLE RESOLVED MULTIPLE WAVELENGTH SCATTEROMETRY TECHNIQUE

Focused beam ellipsometry (FBE) provides a simultaneous measurement of Δ and Ψ , within the range of the incidence angles. It is achieved by focusing a collimated beam onto the sample using the projecting lens with a NA $\sim 0.2-0.3$ or higher and collecting reflected light with a similar lens focused at the same spot. Light beam output from the receiving lens contains light reflected at different angles from the sample at different points across the beam cross-section. Projecting this beam on the array detector, each detector pixel counts photons reflected from

the sample at a different angle of incidence. Figure 1 illustrates the FBE implementation and the principal optical layout of the system.

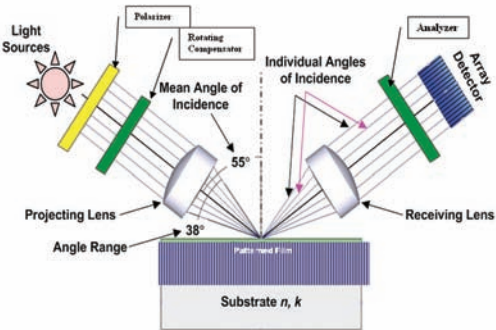


Figure 1 - Focused beam ellipsometry: a collimated beam from the light source is focused at the small spot on the sample by the projecting lens, and reflected light is collected by the receiving lens. The array detector resolves the light scattered at different angles from the sample across the beam cross-section. The polarization state of the incident light is modulated by the rotating compensator.

Data discussed in this paper were obtained using Rudolph Technologies Inc.'s UltraII™ metrology system with the U2CD™ software package. The system allows measurements with light produced by the laser light sources of 633 nm, 780 nm, and 923 nm wavelengths in the range of incidence angles up to 40° with a ~55° mean incidence angle. Two different grating sample orientations—lines either parallel or perpendicular to the ellipsometer incidence plane—can be used for the lines array measurements.

The U2CD™ software package uses the RCWA-based algorithm to calculate the polarization and intensity of the light scattered from the periodic gratings, based on the model of the sample cross-section, incident light wave vector, and polarization state. It provides graphical user interfaces to define and to parameterize a model of the sample cross-section, to analyze measurement sensitivity, and to optimize the measurement configuration for the best measurement speed and precision. U2CD allows either fitting the measured data by non-linear regression or creating a library of the model signals. Non-linear regression is convenient for an initial model optimization; together with the sensitivity analysis, it provides a powerful tool to determine optimal and robust recipe settings for the wavelength and incidence angle ranges to be used, as well as the optimal sample orientation. Library-based lookup and interpolation are used for the fast on-tool measurements,

providing the result in less than 1 sec. The size of the library file varies, depending on applications, from 200Kbytes for a simple two-parameter recipe to 1–2Mbytes for a typical three-parameter library, and up to 50Mbytes for five-parameter libraries.

SAMPLES

The first generation wafer set using the SEMATECH AMAG-5L reticle for optical critical dimension (OCD) evaluation was used in this study. This reticle was designed specifically to evaluate OCD metrology. It includes two-dimensional arrays of 50 μm square gratings, with one axis varying the nominal line widths (scaled to wafer) of 30 nm to 250 nm, mostly in 5–10 nm steps; the second axis of the array varies the pitch ratio for each of these nominal line width sizes, with gratings of nine different pitch ratios from (space:line) 1:1 out to 19:1. All combinations of the following nominal reticle line width and pitch ratio values are thus available:

Scatterometry Gratings of 30, 35, 40, 45, 50, 55, 60, 65, 70, 75, 80, 85, 90, 95, 100, 105, 110, 115, 120, 130, 140, 150, 160, 170, 180, 200, 220, 250 nm (nominal sizes on-reticle, scaled to on-wafer)

Pitch Ratios 1:1, 1.5:1, 2:1, 2.5:1, 3:1, 4:1, 6:1, 9:1, 19:1 (space:line).

To represent an advanced gate lithography process, wafers with 1900 Å thick Sumitomo PAR818 193 nm ArF resist on 770 Å Brewer 29 organic anti-reflective coating (ARC) on 1000 Å amorphous-Si (a-Si) on 20 Å gate oxide were ex-posed on an ASML Twinscan scanner. The wafers were exposed as a focus exposure matrix (FEM) of typical variation. Focus steps were 0.1 μm; exposure steps were 2mJ on the high dose end of the wafer and 1mJ on the low dose end; the lower steps of the higher doses allowed the granularity of the smallest line widths to be fine-tuned before the lines were overexposed to the point of falling over. The center of the exposure window was chosen to intentionally overexpose to reduce feature CDs. A surfactant-assisted developer was used to gain a further process window to smaller line widths. The reticle was the SEMATECH AMAG-5L. Some wafers ended their processing at the resist level, while some were sent through gate etch.

This paper describes measurements on the a-Si etched line arrays of the following dimensions:

Dense: Nominal 80 nm lines with 200 nm pitch, actual size 28 nm–50 nm

Semi-Isolated: Nominal 70 nm lines with 350 nm pitch, actual size 22 nm–45 nm

The resist features varied in size from ~42 nm up through 70 nm, by top-down CD-SEM measurements. The etch, an aggressive trim etch with a 20–25 nm etch delta, yielded decent quality gate lines down to ~30 nm for dense lines with a 200 nm pitch and ~18 nm for isolated lines with a 700 nm pitch. Profiles of the phase-shifted resist structures varied only moderately, while profiles of the etched structures varied minimally. Roughnesses were ~4–5nm for the etched features, although somewhat higher at the extremities of the process window. Similarly, local line width variation was minimal except at the edges of the process window. Different wafers were shot to target isolated lines and dense lines, as the overlap of their process windows was not perfect.

These line arrays are representative of the gate structures for the 90 nm, 65 nm and 45 nm International Technology Roadmap for Semiconductors (ITRS) technology nodes³.

REFERENCE METROLOGY

There are two major considerations for quality reference measurements to correlate to OCD tools. First, OCD tools measure a grating by illuminating it with a beam of light, sampling many repeating features within the grating in a single measurement, and yielding an average measurement. Thus, reference measurements by image-based tools such as CD-SEM or CD-AFM must include many samples over the grating to properly capture the average CD. Second, due to the small precision of OCD tools, the reference measurements of the grating must have a very small (i.e., comparable or better) precision for accuracy and Total Measurement Uncertainty

(TMU)^{1,8} metrics to be meaningful. This requires a large number of CD-SEM or CD-AFM measurements within the same grating structures, as precision will go as $1/\sqrt{N}$ of single measurement precision.

The samples were characterized using CD-AFM and CD-SEM. A detailed description of the procedure can be found in⁴. In summary, the strategy for this study was to use the CD-AFM to calibrate the CD-SEM by measuring the same sites measured with the CD-AFM, and then conducting thorough, 50+ points per grating CD-SEM measurements. Mandel correlations were calculated with the resulting 50+ data pairs. The TMU between the CD-SEM and RMS CD-AFM was found to be ~1 nm for the etched samples. With the CD-SEM calibrated, 50–100 measurements were performed per grating with the CD-SEM. This provided a very high precision of the reference average CD measurement of the grating, ~0.15 nm for the etched wafers. Figure 2 shows example results.

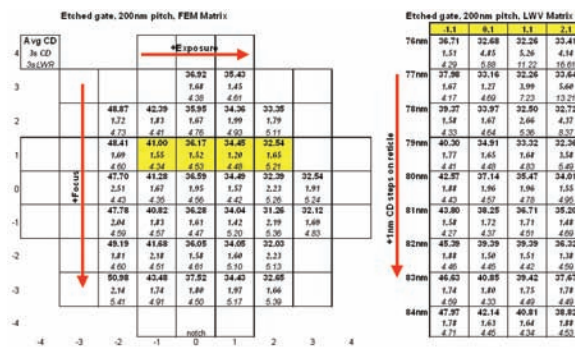


Figure 2 - Reference measurements for the dense (200 nm pitch) etched a-Si gate lines (values reported are CD values at the feature bottom). On the left is the wafer map, showing the reference measurements of the FEM. On right is the line width variation (LWV) matrix. The shaded die in the FEM are those for which the LWV structures were measured. Each measurement included the average CD, 3σ line width variation, and 3σ line width roughness.

The FEM is on the left in Figure 2). Exposure increases to the right, Focus is zero in row 0 and increases positively (re-entrant direction) towards the bottom. On the right are the four die for which line width variation (LWV) array was measured. These four sites correspond to the shaded sites in the FEM. Each LWV die includes 9 gratings, from -4 nm from nominal line width to +4 nm, as denoted by “76nm” through “84nm.” In all cases, the average grating CD, local CD variation (3σ standard deviation of CDs across grating), and 3σ LWR are shown. Reference data were used to optimize the OCD models in an iterative process to minimize TMU^{1,8}.

This paper discusses measurements of the gratings with 200 nm (isolated) and 350 nm pitches (semi-isolated). Thirty-four and 39 die of the FEM wafers were measured for the 200 nm and 350 nm pitch grating arrays, respectively, as some sites were known to be defective and had to be excluded. Measured precision was calculated with five dynamic repeat measurements. Variances of the measured parameters were calculated separately for each measured site on the wafer, and the final precision was obtained as 3 times the square root of the average variance

SENSITIVITY ANALYSIS

Optimization of the measurement and modeling parameters for the best measurement performance starts with the sensitivity analysis, which estimates the changes in the raw data, Δ , Ψ caused by small increments of the grating model parameters—top and bottom CD, line height, pitch, etc.—at different sample orientations and incidence angles. Using characteristics of the measurement noise as input, one can also estimate the precision of the measured structure parameters for a given model of the grating cross-section, with various measurement configurations used to resolve the grating profile and different combinations of fixed, or calculated, parameters. As an illustration, Figure 3 presents the double-trapezoid cross-section model, and Figure 4 shows a simulated measurement signal and its sensitivity to line

height (a-Si_T) and to critical dimensions at the bottom (bot_CD), at the top (top_CD), and in the middle (mid_CD) for the dense a-Si lines. Δ and Ψ values for the incident angles used in the system for each of the three laser wavelengths, are shown in the bottom panel of Figure 4 for two sample orientations: when lines are perpendicular, and parallel to the incidence plane. The latter sample orientation presents a conical diffraction configuration, in contrast with the non-conical configuration where the lines are orthogonal to the incidence plane, which is usually described in the context of measurements performed with the single incidence angle spectroscopic ellipsometry⁵.

The top and center panels of Figure 4 show Δ and Ψ in degrees per 0.1 nm increment of each parameter of the double trapezoid cross-section model. Comparing two graphs, it is reasonable to expect the measurements with lines parallel to the incidence plane of the ellipsometer (top panel Figure 4) to provide better performance, as they are more sensitive to the a-Si line dimensions. This is supported by the estimated parameter precision values, presented in Table 1 for the trapezoid, and double-trapezoid cross-section models, and by different combinations of the fixed and calculated parameters. The measured values of the model parameters’ precision for these models, shown in the same table, further confirm the sensitivity analysis prediction that measured precision is better for the parallel orientation. The accurate quantitative agreement between the measured and predicted precision values is impeded by the facts that first, the sensitivity analysis precision estimates presented here are based on the simplified noise model, assuming the same variability of the measured Δ and Ψ for every incidence angle and for all three wavelengths used in the measurements, and second, measured precision values are averaged over the line arrays with the same line pitch and line height but with the wide range of line CDs from 20 nm to 40 nm across the FEM wafer.

Following this guidance, the rest of the measurements discussed in this paper were performed using lines parallel to the ellipsometer incidence plane.

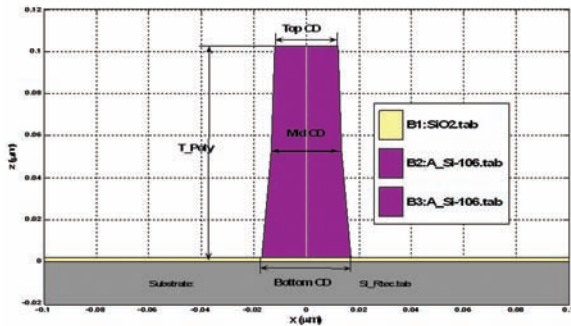


Figure 3 - Double trapezoid cross-section model of the a-Si line array with line pitch=200 nm, a-Si thickness =100.6 nm, top of the line CD=24.2 nm, bottom of the line CD=33.9 nm, mid-CD=26.7 nm, used to generate data shown in Fig.4.

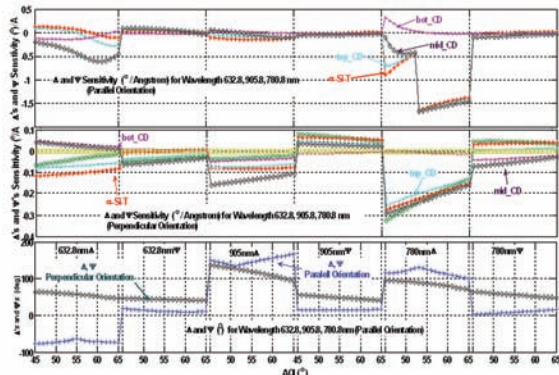


Figure 4 - Modeled data and signal sensitivity for different sample orientations for the a-Si Line array with line pitch=200 nm, a-Si thickness =100.6 nm, top of the line CD=24.2 nm, bottom of the line CD=33.9 nm, mid-CD=26.7nm (Fig.3).

		Estimated stdev 3s (nm)			
		Line Pitch(nm)	poly-T(nm)	top_CD(nm)	bot_CD(nm)
Trapezoid	Orientation	200	98	30	50
	Target Vals	1.324	0.510	0.735	0.674
	Perpendicular	0.718	0.280	0.282	0.232
	Parallel	Fixed	0.477	0.732	0.664
		Measured Precision 3s (nm)			
Perpendicular	Fixed	0.413	0.392	0.359	
Parallel	Fixed	0.289	0.262	0.296	

		Estimated stdev 3s (nm)				
		Line Pitch(nm)	poly-T(nm)	top_CD(nm)	R	mid_CD (nm)
Double trapezoid	Orientation	200	100	24.2	33.9	0.5
	Target Vals	2.341	1.720	5.800	1.486	0.808
	Perpendicular	3.380	0.546	1.542	0.529	0.221
	Parallel	2.327	0.915	2.225	1.428	Fixed
	Perpendicular	3.354	0.375	0.532	0.499	Fixed
	Parallel	Fixed	0.857	1.616	1.969	Fixed
		Measured Precision 3s (nm)				
Perpendicular	Fixed	0.317	0.527	0.484	Fixed	0.214
Parallel	Fixed	0.219	0.702	0.389	Fixed	0.128

Table 1 - Parameter precision estimated by the sensitivity analysis, and actually measured, for two different line cross-section models, different combinations of the fixed and varied model parameters, compared to the measures of precision at two different sample orientations.

RESOLVING DETAILED STRUCTURE PROFILE

Figure 6 shows non-linear regression results for the double-trapezoid model for the 200 nm pitch line array grating on of the die of the FEM wafer. Plots in Figure 5 present measured values of Δ and Ψ vs. incidence angle for three laser wave-lengths, together with the modeled Δ and Ψ curves for the seed and for the final optimized values of the model parameters. Notice that while the initial sensitivity analysis assumed that the narrowest point of the line profile was at the middle of its height, non-linear regression optimization shows that it is in fact closer to the top of the line, at about 80% of the line height. Similar results were obtained for other die across the wafer, and this profile shape was used for the library development, the Mandel Regression precision, and the TMU analysis with the double-trapezoid model. The pro-file cross-section corresponding to the optimized model parameters is shown in the Figure 6 insert.

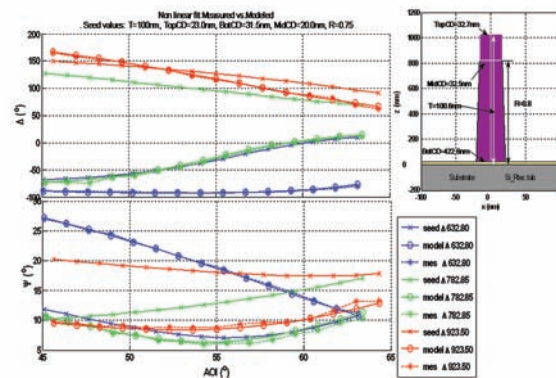


Figure 5 - Example of the line cross-section shape optimized with the double-trapezoid cross-section model. Insert shows the line cross-section profile drawn in scale with the optimized model parameter values. Δ and Ψ plots for three laser wavelengths used in the measurements (632.8 nm, 782.9 nm, and 923.5 nm) show measured values (*) as well as the model values for both seed (X) and optimized (O) model parameter values.

PRECISION AND TMU RESULTS WITH DIFFERENT MODELS

Table 2 compares the precision and TMU of the three types of cross-section models for line arrays with 200 nm and 350 nm pitches. While the fit errors for all three models are practically the same, the trapezoid model provides the best precision and significantly better TMU for the less dense lines. The double trapezoid model, while providing more details about the cross-section profile, does not improve MidCD precision, but improves the TMU.

	Model	Precision 3σ Mid CD (nm)	TMU Mid CD
Line Pitch 200 nm	Rectangle	0.09	0.44
	Trapezoid	0.083	0.54
	Double Trapezoid	0.11	0.48
Line Pitch 350 nm	Rectangle	0.17	1.75
	Trapezoid	0.16	0.83
	Double Trapezoid	0.21	0.66

Table 2 - Precision and TMU from the Mandel regression analysis for the dense (200 nm pitch) and semi-isolated (350 nm pitch) line gratings, analyzed using different profile models. Mid-CD for the trapezoid model is reported as an average of the top and bottom CD values. While the fit errors for all three models are practically the same, the trapezoid model provides the best precision and significantly better TMU for the less dense lines. The double trapezoid model, while providing more details about the cross-section profile, does not improve MidCD precision, but improves the TMU.

EFFECT OF THE OPTICAL PROPERTIES VARIATION

Blanket wafers, with just a flat film of a-Si over the gate oxide over silicon substrate, were used for the initial determination of refractive index at the three laser light wavelengths used in our measurements. However, properties of the a-Si may change during wafer processing, and measurements on some unexposed sites of the etched wafers, where the flat a-Si film remained unetched, showed that the refractive index of the material on the processed wafers is quite different from the blanket wafers. This difference is not small and far exceeds the n and k variability across the wafer (Table 3). To assess the effect of changes in the a-Si properties on the measurement results, we developed another version of the trapezoidal model with the a-Si index values obtained from the processed wafer and remodeled the previously collected measurements. Results showed very little difference in the TMU and precision, but an offset of about 0.5 nm in the

reported mid-CD values. Figure 7 shows the TMU plots for the a-Si line gratings with a 350 nm pitch from the FEM sample wafer. The mid-CD values were obtained using the trapezoid cross-section model with the a-Si refractive index values from the blanket wafer (Fig. 6a) and with the values from the actual processed wafer (Fig.6b). Precision for both models is 0.16 nm, and the TMU is slightly better when the a-Si refractive index values from the etched wafer were used. A difference of up to 4.5% in the refractive index caused a shift of about 0.5 nm in the reported mid-CD.

	Blanket a-Si/Ox/Si	Flat Film a-Si/Ox/Si on the Etched Wafer	
	a-Si Refractive Index	a-Si Refractive Index	Wafer stdev
N633	4.540	4.585	0.0019
K633	0.230	0.246	0.0006
N780	4.160	4.188	0.0013
K780	0.030	0.032	0.0001
N905	4.014	4.038	0.0011
K905	0.021	0.022	0.0001

Table 3 - a-Si refractive index values (N, and K) at the laser wavelengths used in the measurements for the blanket film a-Si/Oxide/Si wafer sample and for the a-Si lines processed wafer, measured, at the unexposed, and unetched areas of the die. The difference is substantial and exceeds the within-wafer variation.

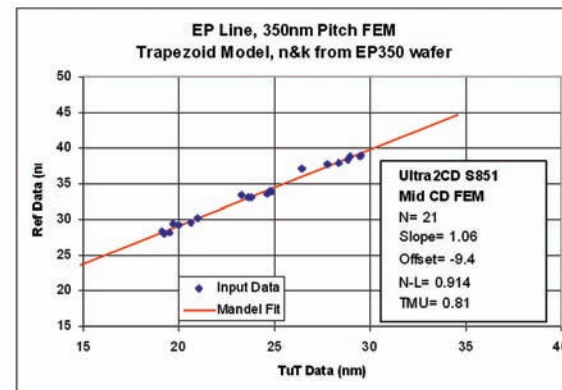
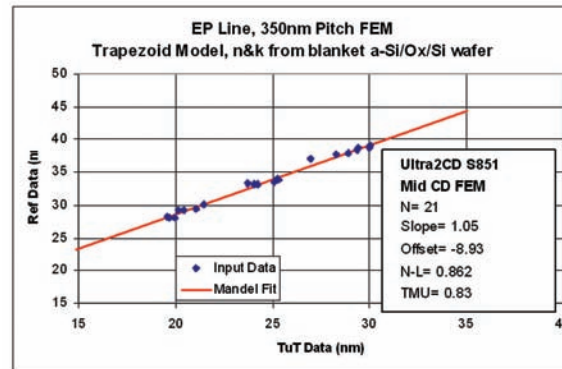


Figure 6 - Mid-CD Mandel regression plots, and TMU for the a-Si line array with 350 nm pitch. The trapezoid model was used with the a-Si refractive index from the blanket a-Si wafer (a) and from the die on the same etched sample wafer.

CONCLUSIONS

Measurements of the etched periodic a-Si line arrays using focused beam ellipsometry have been discussed. Samples were carefully characterized using CD-SEM and AFM as the reference metrology. The measurement precision of the FBE-based measurements exceeded semiconductor manufacturing process metrology requirements for gate control, as outlined in the ITRS³. In contrast with the widely used spectroscopic ellipsometry measurements at a single angle of incidence over a range of wavelengths, the FBE-based technique uses simultaneous measurements at a number of laser light wavelengths, covering a range of incident angles. The most sensitive and precise measurements are at a sample orientation where the periodicity direction of the line array is normal to the incidence plane of the ellipsometer, while the spectroscopic ellipsometry-based CD scatterometry measurements are usually made at the non-conical diffraction geometry with the lines perpendicular to the incidence plane.

We find that the trapezoid cross-section model provided the best precision and TMU performance and that inaccuracy in the refractive index values of the material shifts the reported CD values by few angstroms, but does not significantly affect TMU and precision.

REFERENCES

- ¹ M. Sendelbach and C. Archie, "Scatterometry Measurement Precision and Accuracy Below 70 nm," SPIE: Metrology, Inspection, and Process Control for Microlithography XVII, v5035, pp 224–238, 2003.[OCD_Eval-SPIE_2005]B. Bunday, A. Peterson, and J. Allgair. "Specifications, Methodologies and Results of Evaluation of Optical Critical Dimension Scatterometer Tools at the 90nm CMOS Technology Node and Beyond." Proceedings of SPIE Microlithography, v5752, pp 304-323, 2005.
- ² R. M. A. Azzam and N. M. Bashara, *Ellipsometry and Polarized Light*, 2nd ed. (North-Holland, 1986).
- ³ International Technology Roadmap for Semiconductors, 2006 Update http://www.itrs.net/Links/2006Update/FinalToPost/14_Metrology2006Update.pdf
- ⁴ Benjamin D. Bunday, Osman Sorkhabi, Youxian Wen, Ajit Paranjpe, Paul Ter Beek, John Allgair, and Amy Peterson, Improvement in Total Measurement Uncertainty for Gate CD Control Advanced Characterization Techniques for Optics, Semiconductors, and Nanotechnologies II, edited by Angela Duparré, Bhanwar Singh, Zu-Han Gu, Proceedings of SPIE Vol. 5878 (SPIE, Bellingham, WA, 2005), Proc. of SPIE 58780M-1
- ⁵ X.Niu, N.Jakatdar, S.Yedur, B.Singh, "Specular Spectroscopic Profilometry for the Sub-0.18mm PolySi-Gate Processes," Proc.of SPIE, vol.3998,2000
- ⁶ Richard Silver, Thomas Germer, Ravikiran Attota, Bryan M. Barnes, Benjamin Bunday, John Allgair, Egon Marx and Jay Jun. "Fundamental Limits of Optical Critical Dimension Metrology: A Simulation Study," Metrology, Inspection, and Process Control for Microlithography XXI, edited by Chas N. Archie, Proc. of SPIE Vol. 6518, 65180U, (2007)
- ⁷ T. Novikova, A. De Martino, S. Ben Hatit, and B. Drévilion, "Application of Mueller polarimetry in conical diffraction for critical dimension measurement in microelectronics," Appl. Opt. 45, 3688-3697 (2006).
- ⁸ Benjamin Bunday, Amir Azordegan, Bill Banke, Chas Archie, Eric Solecky, John Allgair, Kye-Weon Kim, Richard Silver. "Unified Advanced Optical Critical Dimension (OCD) Scatterometry Specification for sub-65 nm Technology (2007 version)." ISMI TTID: 04114596D-ENG, Dec 2007. Non-confidential, available on SEMATECH website, <http://www.sematech.org>.

Advanced Materials Research Center, AMRC, International SEMATECH Manufacturing Initiative, and ISMI are servicemarks of SEMATECH, Inc. SEMATECH, the SEMATECH logo, Advanced Technology Development Facility, ATDF, and the ATDF logo are registered servicemarks of SEMATECH, Inc. All other servicemarks and trademarks are the property of their respective owners.